How Gaps are Created during Anticipation of Lane Changes

Chen, Kequan; Knoop, V.L.; Liu, Pan; Li, Zhibin; Wang, Yuxuan

DOI
10.1080/21680566.2022.2152129

Publication date
2023

Document Version
Final published version

Published in
Transportmetrica B: Transport Dynamics

Transportmetrica B: Transport Dynamics

ISSN: (Print) (Online) Journal homepage: https://www.tandfonline.com/loi/ttrb20

How gaps are created during anticipation of lane changes

Kequan Chen, Victor L. Knoop, Pan Liu, Zhibin Li & Yuxuan Wang

To cite this article: Kequan Chen, Victor L. Knoop, Pan Liu, Zhibin Li & Yuxuan Wang (2022): How gaps are created during anticipation of lane changes, Transportmetrica B: Transport Dynamics, DOI: 10.1080/21680566.2022.2152129

To link to this article: https://doi.org/10.1080/21680566.2022.2152129

TRANSPORTMETRICA B: TRANSPORT DYNAMICS
https://doi.org/10.1080/21680566.2022.2152129

Taylor & Francis
Taylor & Francis Group

How gaps are created during anticipation of lane changes

Kequan Chen [a], Victor L. Knoop [b], Pan Liu[a], Zhibin Li[a] and Yuxuan Wang [a]

[a]Department of Transportation, Southeast University, Nanjing, People's Republic of China; [b]Civil Engineering of Technology, Delft University of Technology, Delft, Netherlands

ABSTRACT

The pre-insertion process called anticipation is an essential component of a lane-changing manoeuvre. There is little empirical research regarding the impact of anticipation. Thus, this paper aims to explore the behaviour of the new follower (NF) in the target lane when it encounters anticipation by using new trajectory datasets. The changing magnitude of the reaction pattern is proposed to identify the NF's behaviour. We find that the anticipation significantly affects the NF's movement in terms of gap creation and speed reduction. Then, we conduct a detailed analysis of critical variables to reveal their relationship with the NF's behaviour. Following this, we develop binary logistic models to predict the NF's behaviour, resulting in a good performance. It also suggests that the NF's behaviour is highly related to the anticipation-related variables. The transferability test results show that this model can be directly used in different locations and times with satisfactory accuracy.

ARTICLE HISTORY
Received 13 March 2022
Accepted 22 November 2022

KEYWORDS
Anticipation behaviour; lane-changing impact; car-following behaviour; microscopic trajectory data

1. Introduction

The lane-changing manoeuvre is one of the common driving tasks in traffic streams. In the past 60 years, A large body of studies has been conducted to investigate the lane-changing behaviour (Gipps 1986; Kesting, Treiber, and Helbing 2007; Yang et al. 2018; Gao et al. 2022). More importantly, the previous empirical evidence reported that the impropriety or intensity of the lane-changing manoeuvre is associated with several negative implications. For instance, approximately 5% of traffic accidents in 2015 in China were induced by improper lane-changing manoeuvres (Hou, Edara, and Sun 2015). Yang et al. (2011) showed that the higher frequency of lane-changing behaviour increases the probability and severity of traffic accidents. Previous works have also provided substantial macroscopic evidence that the bottleneck can be activated and lead to a capacity drop due to the high intensity of lane-changing rates (Elefteriadou 1996; Cassidy and Rudjanakanoknad 2005; Patire and Cassidy 2011). In addition, Ahn and Cassidy (2007) contended that the lane-changing manoeuvre significantly affects the formation of traffic oscillation. Zheng et al. (2011a) and Chen et al. (2012a) demonstrated this finding by analyzing the generation of oscillation based on the NGSIM's trajectory data. Zheng et al. (2011b) reported that the lane-changing manoeuvre induces 12 out of 35 traffic oscillations. Since the above studies reported several negative lane-changing impacts on traffic streams, the microscopic-level relationship between the lane-changing manoeuvre and the surrounding vehicles is still unclear (Zheng 2014; Pan et al. 2016). Thus, this paper attempts to provide empirical findings to understand the lane-changing impact.

CONTACT Zhibin Li lizhibin@seu.edu.cn Department of Transportation, Southeast University, Southeast University Road #2, Nanjing 211189, People's Republic of China

In general, a complete lane-changing manoeuvre could be divided into two stages: (1) the anticipation stage and (2) the relaxation stage (Zheng et al. 2013). Specifically, anticipation is used to describe the stage of a lane-changing manoeuvre in which the lane changer (LC) starts to change lanes, but its trajectory is still in the original lane (Li et al. 2020; Chen et al. 2021; Li et al. 2022). Once the LC successfully inserts into the target lane, the LC will experience a relaxation process until its movement is stable in the target lane. The LC will interact with several surrounding vehicles during these two stages, resulting in a complex lane-changing impact.

The relaxation stage has attracted a lot of attention in the literature due to its obvious negative impact (Laval and Daganzo 2006; Carey, Balijepalli, and Watling 2015; Jin 2017; Nagalur Subraveti, Knoop, and van Arem 2019; Yuan et al. 2019). During the relaxation process, the LC is more likely to increase its spacing ahead to a more considerable value larger than the equilibrium value (Smith 1985; Leclercq et al. 2007). This phenomenon was widely noticed after the work of Laval and Leclercq (2008), who proposed a model to describe how the LC and its immediate follower exhibit the relaxation process. Based on this framework, the passing rate of the vehicle was used by Duret, Ahn, and Buisson (2011) to measure the impact of the relaxation. They explained that traffic streams are perturbed by the relaxation process. Oh and Yeo (2015) discussed the lane-changing behaviour in the recovery flow. They revealed that the LC influences the acceleration and deceleration behaviours of the relevant vehicles, which worsens the traffic condition. In addition, the relaxation phenomenon has been considered the primary reason for the capacity drop. Leclercq et al. (2016) provided analytical formulae that focused on the relaxation of the merging vehicle, which can connect the merging behaviour to the capacity value. Chen and Ahn (2018) extended the relaxation of the lane-changing behaviour to investigate how the spatial lane-changing insertion contributed to the capacity drop of merge, diverge, and weaving segments. More recently, Keane and Gao (2021) found that the existing car-following model reacts suddenly at the insertion moment of the lane changer, which is unrealistic. Thus, they proposed a relaxation parameter to smooth the jumping of unmodified headway. This parameter can be incorporated into parametric and non-parametric models.

The above empirical analyses and theoretical models mainly focus on the negative impact of the relaxation phenomenon. As for the anticipation process, Zheng et al. (2013) reported that the new follower (NF) in the target lane may be deviated from its initial driving behaviour to increase the gap for the LC. Here we give a simple example in Figure 1. As we can see from this figure, the NF follows well with the leader (NL) before the LC conducts the lane-changing manoeuvre. After a while, the LC starts to make a lateral moment in the original lane and continually closes to the target lane. The anticipation process ends when the LC inserts into the target lane. Then, the relaxation process follows. This example shows that the NF will adjust its speed and location in response to the LC's anticipation, even though they are not in the same lane. Compared to the analysis of the relaxation phenomenon, anticipation's impact received less attention. Zheng et al. (2013) assumed that the difference between anticipation and relaxation is significantly different but can be captured by one single model. After that, Ghaffari et al. (2015) proposed a novel adaptive neurofuzzy model to simultaneously model the new follower's acceleration during the anticipation and relaxation processes. However, our previous study (Chen et al. 2021) provided several models to find the best way to simulate the lane changer's trajectory. We found that the factors affecting anticipation and relaxation processes are quite different. Additionally, Yang, Wang, and Quddus (2019) examined the NF's reaction and found that about 44% of NFs among 5339 study samples will brake during the anticipation process. Furthermore, the Time to Collision (TTC) value in their study suggested that the NF tends to surface a more risk of rear-end crash in the anticipation process than that in the relaxation process. Despite the negative impact of anticipation on NF's behaviour and safety, available studies on which factors are more likely to induce the NF to change its following behaviour during the anticipation are still lacking.

Thus, this study attempts to answer three challenge problems: (a) Is the NF's behaviour affected by the LC's anticipation process? If so, (b) How the anticipation process affects the NF? Moreover, (c) which factors make the NF more likely to be affected by the anticipation, and can we predict it?

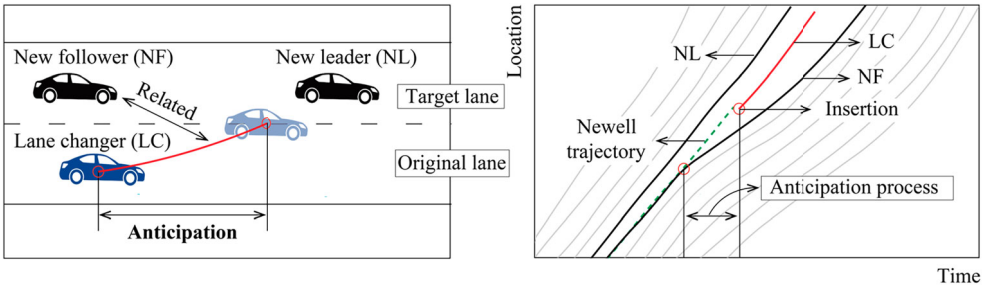

Figure 1. An example of the impact of the anticipation on the new follower's behaviour.

To address the above research questions, we first recorded seven drone videos at three merging bottlenecks in Nanjing, China. The vehicle-level trajectory for each video is automatically extracted. Then, the ratio between the actual wave travel time and theoretical reaction time was used to reflect the NF's behaviour during the anticipation. In this paper, the main contributions are threefold. (a) It provides empirical findings on the impact of anticipation on the NF's following behaviour in terms of gap increase and speed reduction. Empirical findings from large trajectory data are scarce in the existing literature. Still, it is necessary to provide insights into the microscopic details of how the new follower responds to an anticipation process as part of the lane-changing impact. (b) This study is the first attempt to examine which explanatory variables and how they affect the anticipation's impact on the NF. Although some studies reported some negative impacts caused by the lane-changing behaviour, limited available research has discussed which factors and how they contribute to negative anticipation. The statistical analysis in this study is to fill this gap. (c) It applies binary logistic regression to predict the probability of the NF being affected under current traffic environments. It points out that the prediction accuracy can be significantly improved once we consider the anticipation-related factors. This model has been further demonstrated with better performance compared to the state-of-the-art approach and good transferability at different locations and times. The findings and models in this paper fill the knowledge gaps that the previous studies paid little attention to the impact of the anticipation process.

The rest of this paper is organized as follows. Section 2 presents the identification method of driving behaviour. Section 3 presents the preparation of trajectory data. Section 4 presents the empirical results. Section 5 presents the results of binary logistic models. Section 6 presents the conclusions and future works.

2. Methodology

In this section, we adopted the car-following model proposed by Newell (2002) to identify the NF's behaviour during anticipation process of LC. This model assumes that the theoretical trajectory of NF is obtained by shifting the trajectory of NL with a time τ (response time) and a spacing d (minimum stop spacing). For the convenience of discussion, we let i denotes the NF, i-1 denotes the NL, and j denotes the LC in the adjacent lane. Thus, the NF's movement in congestion can be described by:

$$x_i(t) = x_{i-1}(t-\tau) - d \tag{1}$$

where x_i (t) is the position of the NF at time t

The NF's trajectory produced by Equation (1) can be considered the equilibrium trajectory. To measure the NF's real reaction pattern at each time step, we use the method suggested by Laval and Leclercq (2010). It can be shown to be:

$$\eta_i(t) = \tau_i(t)/\tau \tag{2}$$

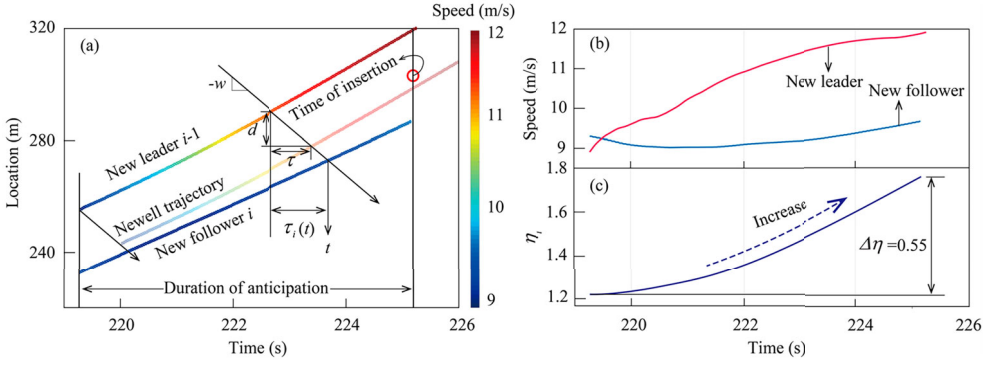

Figure 2. Illustration of the new follower who belongs to group 1: (a) trajectory plots; (b) speed of the new follower and the new leader; (c) reaction pattern curve of the new follower.

where $\tau_i(t)$ is the actual wave trip time of the NF at time t. Thus, the value of $\eta_i(t)$ reflects the ratio of the NF's actual behaviour to the equilibrium at time t.

Based on the value of $\eta_i(t)$, the NF at time t can be identified as aggressive when its $\eta_i(t) < 0.9$, timid when its $\eta_i(t) > 1.1$, and equilibrium when its $\eta_i(t)$ ranges from 0.9 to 1.1 (Chen et al. 2012b; Ma and Qu 2020). Recall that we are interested in how the NF responds to the anticipation process. Therefore, we quantify this via the changing magnitude of $\eta_i(t)$ at the start and end moments of the anticipation process, which can be computed as follow:

$$\Delta\eta_i = \eta_i(T_e) - \eta_i(T_s) \tag{3}$$

where T_s and T_e are the start and end moments of the anticipation process, respectively. We will introduce how to determine these two moments in Section 3.

It is clear that $\Delta\eta_i$ will be positive if the NF attempts to deviate from its initial state. On the contrary, it will be negative if the NF attempts to reduce its initial state. Therefore, it is possible to classify these two distinct behaviours into two groups in terms of the value of $\Delta\eta_i$. Specifically, the NF i belongs to group 1 if $\Delta\eta_i \geq 0.1$, and it belongs to group 2 if the $\Delta\eta_i < 0.1$. The threshold of 0.1 is determined since the slight fluctuation of the reaction pattern can be considered the driver's inherent influence (Chen et al. 2012a).

Here, we give the first example in Figure 2 to illustrate the NF's behaviour in group 1. As shown in Figure 2(a), the actual trajectory of the NF is gradually far away from the Newell trajectory before the insertion moment of the LC. Particularly, the NL accelerates from 8.82 m/s to 11.8 m/s, whereas the NF still maintains a lower speed, around 9 m/s. As a result, a large gap is created for the insertion of the LC; see Figure 2(b). In addition, Figure 2(c) displays the reaction pattern of the NF. From this figure, we can observe that the $\eta_i(t)$ gradually increases from 1.22 to 1.78, even though the NF's initial behaviour is timid. This is a representative example in which the NF's behaviour is somehow affected.

On the contrary, we also show another case in Figure 3 where the value of $\Delta\eta_i$ equals -0.72. From the trajectory and speed plots in Figure 3(a,b), we can find that the NF tries to reduce the spacing ahead. As a result, the NF's trajectory returns towards the equilibrium state, which can be observed from the curve of the reaction pattern in Figure 3(c). Since we assume that the driver's natural behaviour is to return to the equilibrium state, this typical example suggests that the NF seems to maintain its following behaviour during the anticipation process.

3. Preparation of trajectory data

In this section, we introduce the preparation of trajectory data for investigating the NF's response to the anticipation process. Three merging bottlenecks are selected in Nanjing city, China. Figure 4 shows

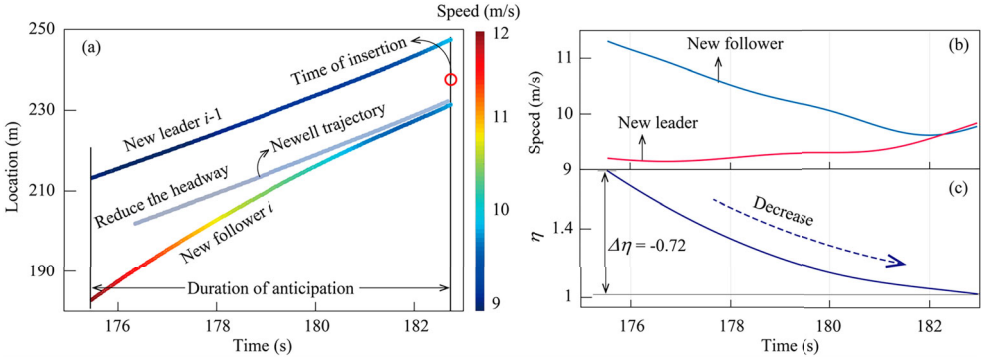

Figure 3. Illustration of the new follower who belongs to group 2: (a) trajectory plots; (b) speed of the new follower and the new leader; (c) reaction pattern curve of the new follower.

Figure 4. Structure of three merging bottlenecks.

the structure of these three merging bottlenecks, namely 'site 1', 'site 2', and 'site 3', respectively. Then, a drone was used to record videos. The drone carries a 4 K resolution camera, which can provide us with a high definition (3840 $\times$ 2160) and 30 frames per second (fps) video. Ultimately, we recorded three times, two times, and two times videos at site 1, site 2, and site 3 during the morning peak hours, respectively. Table 1 presents the information for the seven videos. After we got the drone videos, we adopted an automatically trajectory extraction framework to extract the vehicle-level trajectory for each video. The read is referred to our previous studies for a detailed information of this method (Wan et al. 2020; Chen et al. 2021). Generally, this trajectory extraction method includes four steps: (1) vehicle detection, (2) vehicle tracking, (3) lane detection, and (4) raw data smoothing. To ensure the vehicle detection accuracy at different locations, we further trained the detecting layer with several traffic flow scenarios, such as the merging, diverging, weaving, intersection, and basic road segments

Table 1. The detailed information of seven datasets.

Trajectory datasets	Study site	Date	Time	Weather	Road length (m)	Average speed (m/s)	Average density (vehicle/km)
Dataset 1	Site 1	15 December 2020	7:30 am—7:45 am	Sunny	340	9.09	212
Dataset 2	Site 1	17 December 2020	7:30 am—:55 am	Sunny	320	7.22	235
Dataset 3	Site 1	15 April 2021	7:30 am—8:00 am	Sunny	420	11.56	184
Dataset 4	Site 2	8 May 2021	7:40 am—7:55 am	Sunny	400	8.95	201
Dataset 5	Site 2	9 May 2021	7:30 am—8:20 am	Sunny	360	5.02	248
Dataset 6	Site 3	17 August 2021	7:30 am—8:05 am	Sunny	400	9.47	206
Dataset 7	Site 3	19 August 2021	7:35 am—8:00 am	Sunny	390	7.67	229

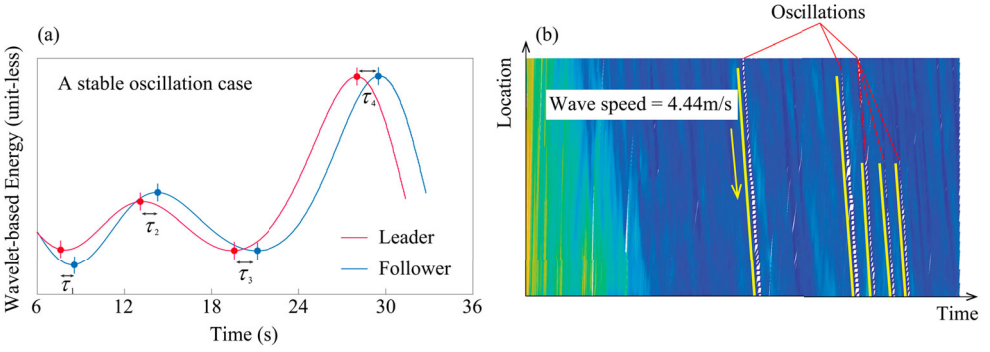

Figure 5. Calibration of critical parameters (a) response time; (b) wave speed.

during the daytime and nighttime. Consequently, we got a strong detecting network that achieve satisfactory accuracy at different bottlenecks. Specifically, this extraction method provides us with the following vehicle-level information: lane number, vehicle ID, time (1/30s interval), lateral position (m), longitudinal position (m), speed (m/s), and acceleration (m/s^2). Finally, we obtained seven high-quality trajectory datasets. The average speed and density for each trajectory dataset are also shown in Table 1.

Based on the trajectory data, we apply the Wavelet-transform method recommended by Zheng et al. (2011b) to calibrate the response time τ and the wave speed w. Figure 5(a) shows an example where the speed of the NF and its leader have been transformed into wavelet energy distribution. The abruptness of this energy represents the speed change moment. Consequently, the time difference of the energy abrupt between two adjacent vehicles can be determined as the response time. In this simple example shown in Figure 5(a), we can obtain four response time samples. Without loss of generality, we select 200 samples from 12 stable oscillations. The average value of these samples as τ (1.3 s) is used for all the NFs. Next, we determine the wave speed w based on the average slopes of the 12 stable oscillations. We illustrate some oscillation cases in Figure 5(b). Once we have the wave speed w ($w = 4.4$ m/s) and the response time τ, we can compute the minimum stop distance d through $d = \tau^* w$ ($d = 5.7$ m).

Recall that we aim to investigate the NF's response and its relationship with the anticipation process. Thus, only the anticipation samples inducing the LC's anticipation process and its corresponding trajectories of the NF and NL in the target lane are helpful for the following analysis. To obtain such sample, we first need to determine two critical time points: the start moment and the end moment of the anticipation process (denoted as T_s and T_e, respectively). We give two examples in Figure 6. The detailed procedures for detecting these two moments are presented as follows:

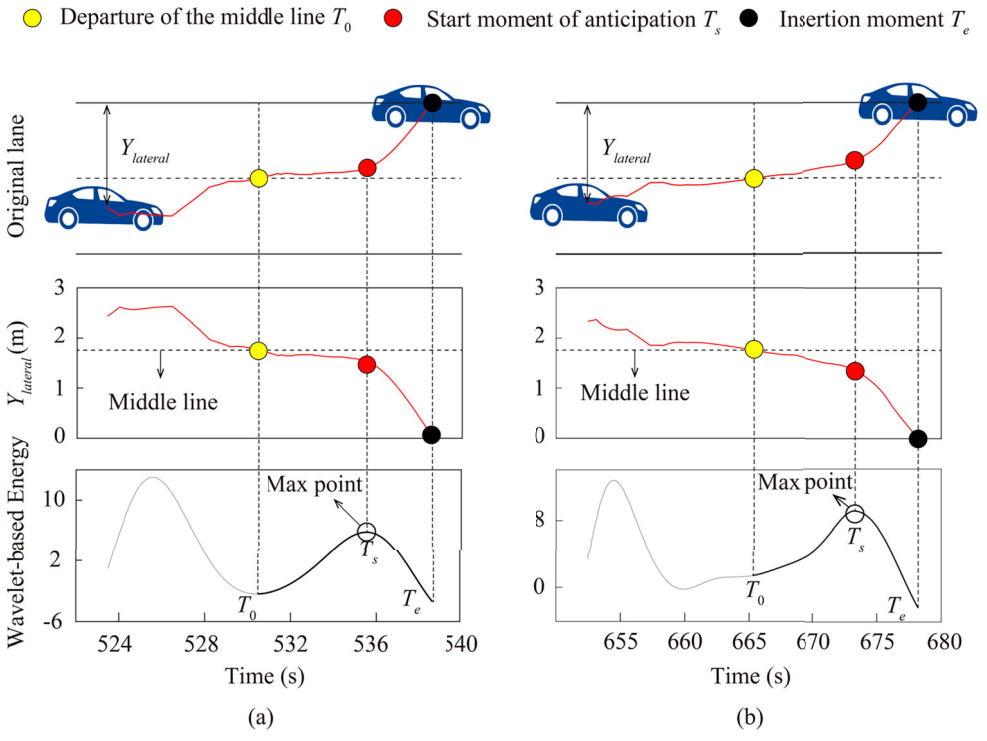

Figure 6. The measurement of the start and end moments for the anticipation (a) case 1, (b) case 2.

- The moment when the LC departs the middle line of the original lane is located as T_0; see the yellow cycle in Figure 6.
- When the LC's lateral distance to the target lane edge ($Y_{lateral}$) equals 0, we can locate this time as the end moment of the anticipation process (T_e); see the black cycle in Figure 6.
- The start moment of the anticipation (T_s) is between T_0 and T_e. In the previous studies (Ali, Zheng, and Haque 2018; Yang, Wang, and Quddus 2019), the time T_s is located once we observe a drastically change of the LC's lateral movement. To pinpoint such sudden lateral change, we adopt the Wavelet-transform method, which has been successfully used to detect the singularities in the traffic data. As shown in the lower part of Figure 6, the LC's lateral movement has been transformed into wavelet-based energy. The max point of the wavelet-based energy between T_0 to T_e is marked as the T_s; see the red cycle in Figure 6.

The above procedures are used to extract the anticipation samples out of all seven trajectory datasets. After that, we got 4698 anticipation samples. Note that we observe that all these samples can be split into four cases: (1) the NF speeds up the LC (231 samples), (2) the LC speeds up the NL. Then the NL becomes the new NF after the insertion (424 samples), (3) the NF or the NL also changes its lane (203 samples), and (4) the NF and the NL are both the same vehicles for the whole duration of anticipation process (3840 samples). We employ the fourth case for the following analysis in this study for two reasons: (1) the majority proportion of anticipation samples is the fourth case (about 82%), and (2) the unchanged follower is suitable for analyzing its following behaviour during the anticipation. Here, we give four examples of available anticipation samples in Figure 7. As we can see that one study sample should include the LC's anticipation process, which starts at T_s and ends at T_e (red dotted line), and its consistent NF (green line) and NL (blue line)

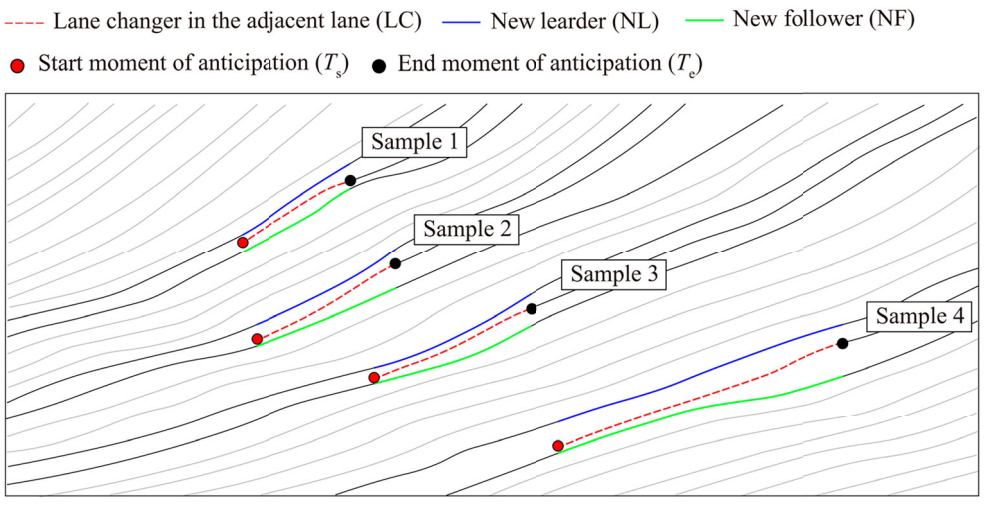

Figure 7. Illustration of study samples.

Table 2. The classification results.

	Study samples in group 1	Study samples in group 2	Total
Site1	1215	588	1803
Site2	683	309	992
Site3	714	331	1045
Total	2612	1228	3840

4. Empirical results

This section presents empirical results to understand NF's behaviour during the anticipation process. We start by describing the classification result of NF's behaviour (Section 4.1). Then, the impact of NF's behaviour on the gap increasing value and speed reduction in the target lane is investigated (Section 4.2). Additionally, we examine some particular relationships in more detail, such as the relationship between the NF' behaviour and two headways (in s): (1) headway between the NF and NL; and (2) headway between the NF and LC (Section 4.3), the relationship between NF's behaviour and the headway between NF and LC versus the LC's speed (Section 4.4).

4.1. Classification result

According to the behaviour analysis method described in Section 2, we first divide all the 3840 study samples into group 1 and group 2. The classification result is shown in Table 2.

To investigate the changing amplitude of the reaction pattern in two groups, we start the analysis by showing the reaction pattern value at the start moment of anticipation $\eta(T_s)$ and the end moment of the anticipation $\eta(T_e)$ in Figure 8(a). The corresponding descriptive statistic is displayed in Table 3. As we can see from this figure, the average value of $\eta(T_s)$ is 1.22 and 1.69 in group 1 and group 2, respectively. ANOVA test is applied, and the test result shows that the initial value of the reaction pattern in group 1 is significantly lower than that in group 2. After the anticipation process, the reaction pattern value increases to the average value of 1.78 in group 1 and reduces to that of 1.15 in group 2. The detailed distribution of $\Delta\eta_i$ for the two groups is shown in Figure 8(b). The above results for group 1 highlight that even though the NF's initial reaction pattern value is larger than the equilibrium value, the NF still tends to be away from the equilibrium state. Since the LC is conducting an anticipation

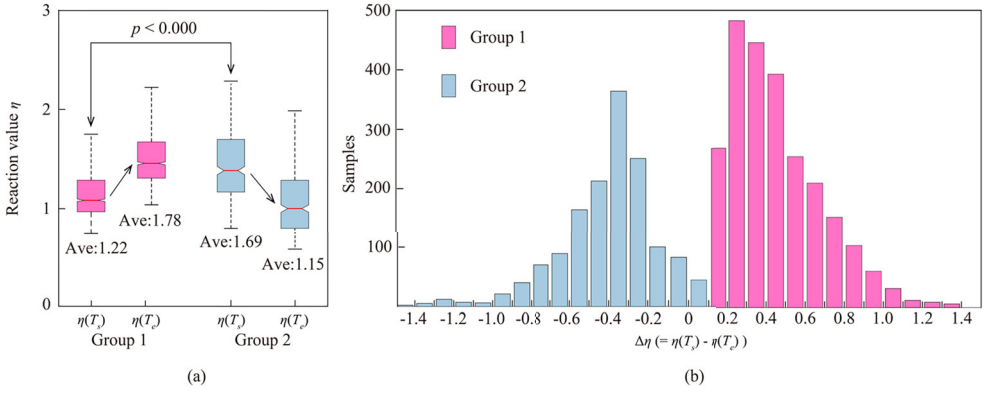

Figure 8. The changing magnitude of the reaction pattern of new followers in group 1 and group 2.

Table 3. Description results of the reaction pattern for group 1 and group 2.

	Mean	Std	Min	Max
Group 1				
$\eta(T_s)$	1.22	0.31	0.76	3.12
$\eta(T_e)$	1.78	0.32	0.92	3.34
$\Delta\eta$	0.56	0.14	0.11	1.35
Group 2				
$\eta(T_s)$	1.69	0.57	0.82	3.33
$\eta(T_e)$	1.15	0.54	0.75	3.16
$\Delta\eta$	−0.54	0.20	−1.38	0.09

Note: The mean values in group 1 are significantly different from group 2 in the ANOVA test ($p < 0.001$).

process in the adjacent lane and tries to insert ahead of the NF, it is natural to assume that the NF's behaviour is related to the anticipation. We will further discuss this assumption in Section 4.3.

Additionally, the decreasing trend of $\Delta\eta_i$ in group 2 is reasonable since the driver's task always tends to return to equilibrium if the initial value is relatively large. This also seems to suggest that some NFs will not adjust their following behaviour when they notice an anticipation process happening in the adjacent lane. After the above classification and description results on the NF's reaction pattern, we continue with the investigation of how the gap in the target lane and the speed of NF change in these two groups.

4.2. Impact of anticipation

This subsection investigates the anticipation's impact on the changing of gap size and speed fluctuation. First of all, we define ΔS to reflect the changing magnitude of the gap between NF and NL after the NF experiences an anticipation process, which can be computed as below:

$$\Delta S = \Delta S_{NL-NF}(T_e) - \Delta S_{NL-NF}(T_s) \tag{4}$$

where $\Delta S_{\text{NL-NF}}(T_s)$ and $\Delta S_{\text{NL-NF}}(T_e)$ are the gap between NF and NL at the start and end moments of the anticipation, respectively.

Figure 9 shows the distributions of ΔS in group 1 and group 2, and their statistical results are given in Table 4. We can clearly observe that the distributions of ΔS are quite different in group 1 and group 2. Specifically, the distribution of ΔS is concentrated around the positive axis in group 1 and around the negative axis in group 2. The results coincide with the definitions of group 1 and group 2. Moreover,

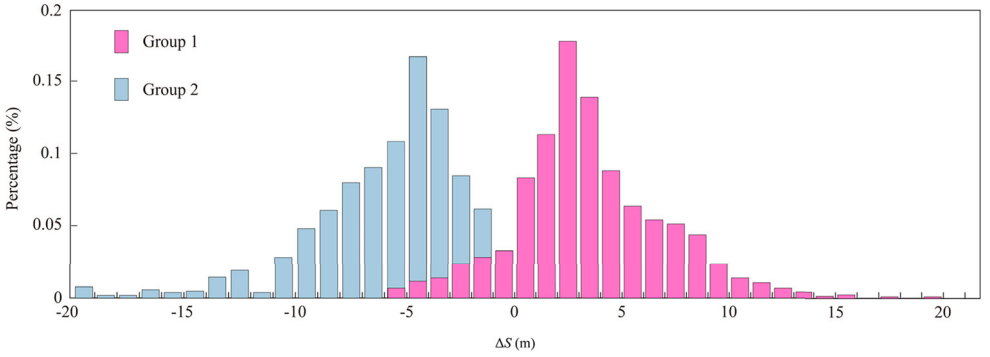

Figure 9. Gap changing distributions for group 1 and group 2 after anticipation.

Table 4. Descriptive results of the gap changing distribution.

	Mean	Std	Min	Max
ΔS in group1	5.36	4.65	−6.38	20.31
ΔS in group2	−4.65	6.31	−19.32	2.13

Note: The mean values of Delta S between group 1 and group 2 are significantly different in the ANOVA test ($p < 0.001$).

the statistical result of group 1 in Table 4 shows that if the anticipation affects the NF's behaviour, an extra gap (mean value = 5.36 m) between the NF and NL will be induced.

Next, we turn our attention to the speed fluctuation in two groups. Let us denote $\Delta\varphi_{NL}$ and $\Delta\varphi_{NF}$ as the speed-changing value of the NL and the NF after anticipation, respectively, which can be written as:

$$\Delta\varphi_{NL} = V_{NL}(T_e) - V_{NL}(T_s) \tag{5}$$

$$\Delta\varphi_{NF} = V_{NF}(T_e) - V_{NF}(T_s) \tag{6}$$

where V_{NL} (T_s) and V_{NL} (T_e) are the speed of NL at the start and end moments of the anticipation process, respectively, V_{NF} (T_s) and V_{NF} (T_e) are the speed of NF at the start and end moments of the anticipation process, respectively. Generally, if the NF is in an equilibrium state, the speed-changing value of NF will approximately equal to that of NL. Thus, the difference value between $\Delta\varphi_{NL}$ and $\Delta\varphi_{NF}$, denoted as $\Phi = \Delta\varphi_{NF} - \Delta\varphi_{NL}$, is capable of reflecting how the NF responds to the anticipation process.

Figure 10 shows the distributions of Φ in group 1 and group 2. The descriptive statistic results of these distributions are displayed in Table 5. The result for group 1 in Table 5 suggests that the NL is more likely to accelerate (mean = 0.63 m/s), while the NF tends to decelerate (mean = −0.23 m/s) during the anticipation process. As a result, the distribution of Φ in group 1 is concentrated on the left side of zero; see Figure 10. These distinct driving behaviours of NL and NF explain how the gap created in the target lane. Regarding group 2, the average value of $\Delta\varphi_{NL}$ is −1.58 m/s, suggesting that the NL in group 2 is more likely to decelerate during the anticipation. Meanwhile, the average value of $\Delta\varphi_{NF}$ (−0.89) is smaller than that of $\Delta\varphi$L. Marczak, Daamen, and Buisson (2013) reported a similar finding. This finding explains the formation mechanism of group 2, which is that the NL tends to decelerate while the NF exhibits a slower response. As a result, the NF's reaction pattern value is reduced.

The above findings report that the consequences of NF in group 1 are clearly different from that in group 2 regarding gap creation and speed reduction. Thus, an interesting problem lies in whether we can find multiple factors that directly describe the NF's behaviour during the anticipation process.

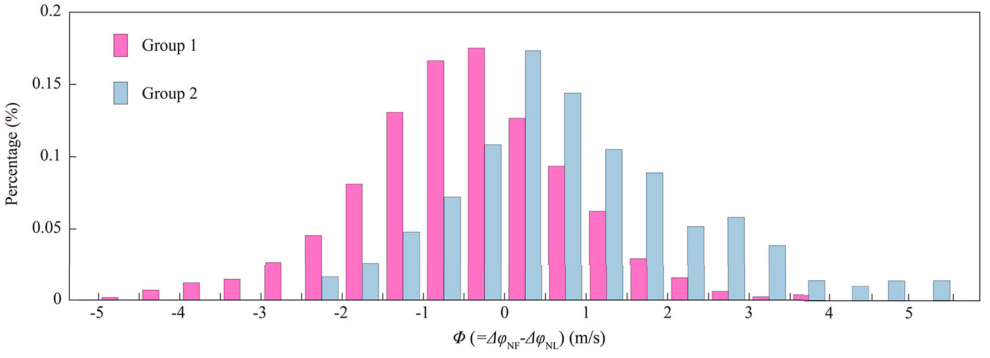

Figure 10. Distribution of the difference in speed fluctuation between the new follower and its leader for group 1 and group 2.

Table 5. Descriptive results of the speed changing distribution.

	Mean	Std	Min	Max
Group 1				
$\Delta\varphi_{NL}$	0.63	1.83	−10.63	7.66
$\Delta\varphi_{NF}$	−0.23	1.60	−11.24	7.00
Φ	−0.80	1.53	−4.85	4.59
Group 2				
$\Delta\varphi_{NL}$	−1.58	2.68	−14.73	5.87
$\Delta\varphi_{NF}$	−0.89	2.19	−13.24	7.60
Φ	0.69	1.66	−3.26	5.23

Note: The mean values in group 1 are significantly different from group 2 in the ANOVA test ($p < 0.001$).

4.3. Relation between headways and the follower's behaviour

This subsection investigates whether these two groups' headway (in s) between the NF and NL (T_{NF-NL}) is different. The ANOVA test and the distribution of T_{NF-NL} in two groups are displayed in Figure 11. The results show that T_{NF-NL} has no significantly different in group 1 and group 2 ($p = 0.52$). Therefore, one could argue that the difference in NF's behaviour is not a difference in its present headway with the NL. Furthermore, we compare the headway (in s) between the NF and the LC (T_{NF-LC}) in group 1 and group 2; see Figure 12. We can see that the value of T_{NF-LC} in group 1 is significantly smaller (1.45s) than that in group 2 (2.12s). This finding would be evidence that the relation between the NF and LC significantly affects the NF's behaviour. This is easy to understand that when the LC conducts an anticipation process with a smaller headway with NF, the NF is more likely to adjust its speed and location to ensure safety.

4.4. Anticipation speed versus follower's behaviour and headway

Figure 13 presents the result of the relation between the anticipation speed (V_{LC}) and the NF's behaviour. Note that the anticipation speed here is defined by the LC's speed at the start moment of the anticipation process. The ANOVA test result is presented in Figure 13(a). It suggests that the V_{LC} at group 1 and group 2 are significantly different ($p < 0.000$). The V_{LC} in group 1 (mean = 5.82 m/s) is smaller than that in group 2 (mean = 9.59 m/s). This result reveals that the NF tends to deviate from the initiate reaction pattern if the LC conducts the anticipation with a lower speed. Since the NF in group 1 is more likely to suffer slow anticipation speed and small headway value of T_{NF-LC}, we compared the relationship between the anticipation speed and the headway T_{NF-LC}. The comparison

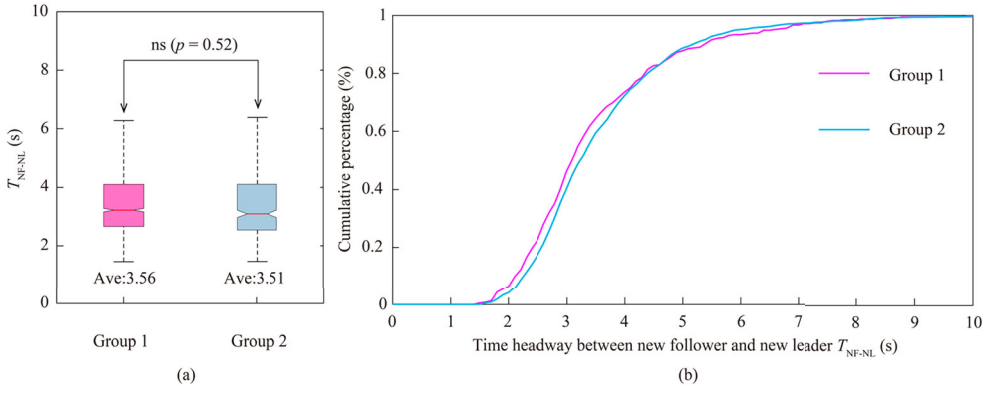

Figure 11. Relation between the time headway (new follower and new leader) and the new follower's behaviour.

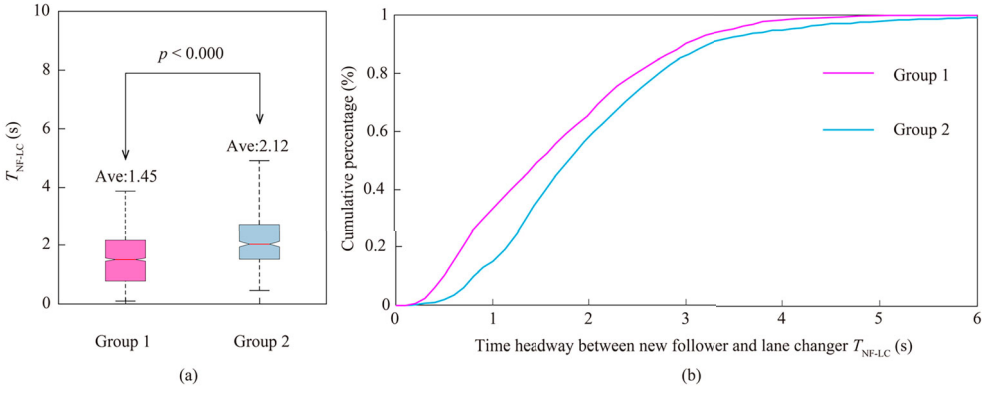

Figure 12. Relation between the headway (new follower and lane changer) and the new follower's behaviour.

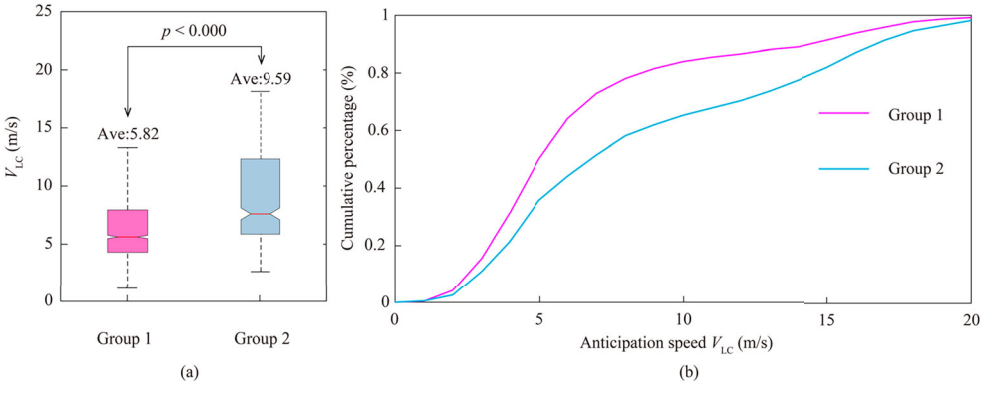

Figure 13. Relation between anticipation speed and the new follower's behaviour.

result is shown in Figure 14. This figure shows a large variance and a small value of the Pearson correlation coefficient (0.09). This finding reveals that it is impossible to identify the anticipation speed based on the value of headway between the LC and the NF.

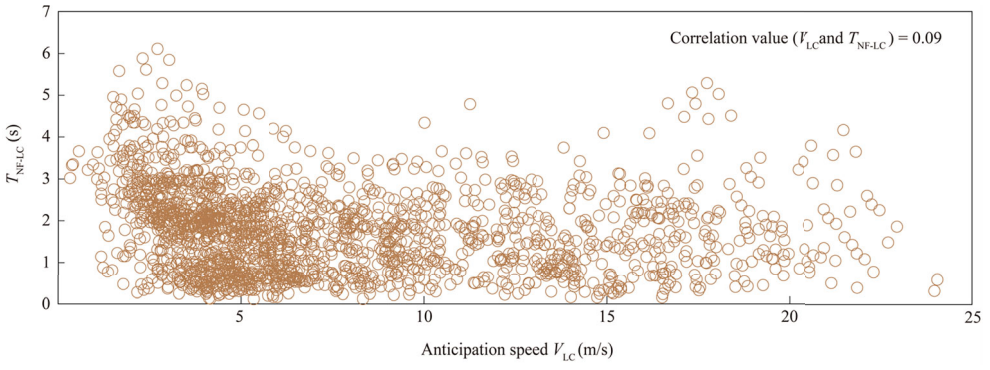

Figure 14. Relation between anticipation speed and headway between new follower and lane changer.

5. Binary logistic regressions: which factors influence new follower's behaviour during anticipation

In this section, we first develop binary logistic regressions in Section 5.1 to predict the new follower' behaviour during the anticipation. In Section 5.2, we calibrate and test the performance of the developed models. Moreover, we compare our model with the model proposed by Zheng et al. (2013) in Section 5.3. Finally, we further collected four trajectory datasets under different bottlenecks and times to examine the transferability of the developed model in Section 5.4.

5.1. Model development

As for the approach to model the lane-changing behaviour, non-parameter and parameter models are widely used in previous studies. The non-parameter method, such as deep learning method (Zhang et al. 2022), and data-driven simulation (Liu et al. 2022) have been developed to predict lane-changing behaviour. However, these non-parameter models mainly focused on improving the predicted accuracy of lane-changing decisions instead of understanding the lane-changing impact on the target lane. The parameter models such as the multilevel linear regression model (Yang, Wang, and Quddus 2019), the linear mixed model (Ali, Zheng, and Haque 2018), and the binary model (Ng et al. 2020) have been used to connect factors to the lane-changing behaviour. Our work aims to quantify the multiple factors on the probability of whether the NF changes its following behaviour when the anticipation occurs in the adjacent lane. Considering the fact that whether the NF changes its following behaviour is a binary problem, the binary logistic regression is selected to fill this need.

Let the dependent variable Y = 0 represent the NF who belongs to group 1, and Y = 1 represents the NF who belongs to group 2. Then, we set an input vector X_n to represent the initial relationship among three vehicles: NF, NL, and LC, where the subscript n is the number of candidate variables. Thus, the general formulation of the binary logistic regression can be expressed as below:

$$\Pr(Y = 0|X_n) = \frac{\exp[f(X_n, \beta)]}{1 + \exp[f(X_n, \beta)]} \tag{7}$$

where $\Pr(Y = 0|X_n)$ is the probability that the NF belongs to group 1 if the LC conducts the anticipation process at the initial state of X_n; $f(X_n, \beta)$ is the multiple linear regression function which can be written as Equation (8):

$$f(X_n, \beta) = X_n\beta_n + \beta_0 \tag{8}$$

where β_n is the coefficient, and β_0 is the constant.

Based on this framework, we develop two models. The first model only considers the relation between NF and NL (model 1). The second model is constructed by adding the anticipation-related

Table 6. Pearson's correlation coefficients between all the candidate variables.

	1	2	3	4	5	6	7
1. New follower's speed (XV_{NF})	1						
2. Relative speed between new follower and new leader (XV_{NL-NF})	−0.13	1					
3. Initial reaction pattern of the new follower ($X\eta(T_s)$)	0.12	−0.16	1				
Anticipation-realted variables							
4. Anticipation speed (XV_{LC})	0.82	0.06	0.17	1			
5. Relative speed between lane changer and new follower (XV_{LC-NF})	−0.14	0.18	−0.14	0.15	1		
6. Headway between new follower and lane changer (T_{NF-LC}).	−0.03	0.02	0.05	−0.03	0.08	1	
7. Relative speed between new leader and lane changer (XV_{NL-LC})	0.03	0.11	0.09	−0.10	0.05	−0.12	1

variables into model 1 (model 2). Specifically, three factors which are the speed of NF (XV_{NF}), the relative speed between NF and NL (XV_{NL-NF}), and the initial reaction pattern of NF ($X\eta(T_s)$), are considered in model 1. As discussed in Section 4.3, the headway between the NF and NL is not significantly different in these two groups. Thus, we do not consider this variable in model 1. On the other hand, we construct model 2 by incorporating four additional anticipation-related variables into model 1, which are the anticipation speed (XV_{LC}), the relative speed between LC and NF (XV_{LC-NF}), the headway between the NF and LC (T_{NF-LC}), and the relative speed between NL and LC (XV_{NL-LC}). Comparing these two models helps us understand whether the anticipation-related variables can increase the prediction accuracy.

5.2. Models results

Multicollinearity among the above variables has been first checked using Pearson's correlation coefficient (PCC). Table 6 presents their PPC values. From this table, there are two observations to be highlighted. Firstly, the PPC value between XV_{NF} and XV_{LC} is particularly large (0.82), suggesting that the speed of the NF has a positive correlation with that of the LC. Thus, the variable XV_{NF} is removed in the construction of model 2. Secondly, the rest of these independent variables produce PPC values between −0.14 and 0.18. Then, we can conclude that the selected independent variables in the two models exclude any serious multicollinearity.

Table 7 presents the estimation results for model 1 and model 2. In this table, one observes that the coefficient of $X\eta(T_s)$ is negative. This result suggests that a smaller initial reaction pattern value of NF increases the probability that NF's behaviour belongs to group 1, which is coincident with the ANOVA test result in Figure 8(a). As expected, the coefficient of XV_{NL-NF} is positive, which means the higher speed of NL than that of NF, the higher the probability for the NF to deviate from its initial behaviour. This finding seems reasonable because the NF will fall behind if a larger speed difference exists between NL and NF. However, all the samples in this study were collected in congested traffic conditions; see the mean speed value in Table 1. Leaving aside the setting of timid or aggressive behaviours, the NF's natural behaviour is to follow its leader and maintain an equilibrium state as much as possible. Nevertheless, the discussion in Figure 10 suggests that the NF tends to decelerate even though the NL accelerates during the anticipation process, which is opposite to the typical driving experience. Thus, it may be incomplete to determine the NF's behaviour only based on the relation between NF and its leader.

The estimation results of model 2 are also shown in Table 7. From this table, the impact trends of $X\eta(T_s)$ and XV_{NL-NF} are the same as in model 1. Moreover, the negative coefficients of T_{NF-LC} and XV_{LC} are observed, coinciding with the discussion in Figures 12 and 13, respectively. The negative coefficient of XV_{LC-NF} suggests that the probability that the NF's behaviour belongs to group 1 will be increased with the reduction of the speed difference between LC and NF. It reveals that if the LC's anticipation speed is lower than NF, the NF is more likely to decelerate to ensure safety with the LC. The finding further explains that the deceleration behaviour of the NF is related to the anticipation speed. Finally,

Table 7. The estimation and fit results for model 1 and model 2.

Variables	Description	Model 1 Coefficient	Model 1 Standard error	Model 2 Coefficient	Model 2 Standard error
$X\eta(T_s)$	Initial reaction pattern of the new follower	−1.93***	0.24	−1.72***	0.28
XV_{NL-NF}	Relative speed between new follower and new leader	1.54***	0.12	0.78***	0.12
XV_{NF}	New follower's speed	−0.09***	0.04	–	–
Anticipation-related					
XV_{LC}	Anticipation speed	–	–	−0.13***	0.02
XV_{LC-NF}	Relative speed between lane changer and new follower	–	–	−1.95***	0.09
T_{NF-LC}	Headway between new follower and lane changer	–	–	−0.52***	0.15
XV_{NL-LC}	Relative speed between new leader and lane changer	–	–	1.45***	0.07
Intercept		4.73***	0.22	5.23***	0.35
Model fit statistics					
No. of parameters		4		7	
No. of observations		3840		3840	
Log-likelihood at zero		−1083.17		−1186.54	
Log-likelihood at convergence		−711.56		−506.75	
Likelihood ratio test χ^2		371.61		679.79	
McFadden's ρ^2		0.40		0.62	
BIC		1456.13		866.55	

***Significant at $p < 0.001$.

the coefficient of XV_{NL-LC} is positive, indicating that the probability of the NF's behaviour belonging to group 1 increased with the increase of the speed difference between NL and LC. This finding might seem strange, but it can be explained that the NF changes the following target to the LC when it notices the anticipation process. Then, the NF may slow its speed if the LC's speed is lower than the NL's speed.

To further measure the performance of these two models, we calculate three commonly accepted fit statistics (Schwarz 1978; Roque, Moura, and Lourenço Cardoso 2015; Wang et al. 2020): (1) McFadden's ρ^2; (2) Likelihood ratio test χ^2; (3) Bayesian Information Criterion (BIC). One model with higher values of Likelihood ratio and McFadden's ρ^2, lower value of BIC is preferred. Table 7 presents the comparison results for model 1 and model 2. We can clearly see that model 2 provides a significantly better fit than model 1. McFadden's ρ^2 in model 2 is 0.62, indicating that the selected six independent variables with one constant can explain about 62% of the variation in the dependent variable. While model 1 can only explain about 40% of the variation in the dependent variable.

A confusion matrix is adopted to examine the prediction accuracy. In general, a confusion matrix includes four essential elements, which are (1) true positive (TP), (2) false positive (FP), (3) true negative (TN), and (4) false negative (FN). Based on the four factors, the recall and the false alarm rate (FAR) are computed to evaluate the minority and majority classes, respectively. The recall indicates how many samples in group 1 are correctly detected out of all the group 1 samples. The FAR indicates how many samples in group 2 are wrongly detected as group 1 out of all the group 2 samples. The Receiver Operating Characteristic curve (ROC) curve is constructed in which the horizontal axis represents the FAR, and the vertical axis represents the recall. Note that the threshold to compute the ROC increases from 0 to 1 with an interval of 0.1. The area under the ROC (AUC) is calculated to evaluate the classification capable between group 1 and group 2. The detailed results for model 1 and model 2, including the confusion matrix, recall, FAR, and AUC, are provided in Table 8. The results indicate that the prediction capability of model 2 outperforms model 1.

In summary, the results of Tables 7 and 8 conclude that these four anticipation-related variables play a vital role in increasing the prediction accuracy of whether the NF changes its behaviour during the anticipation process. NF's behaviour can be better predicted when we consider these four anticipation-related variables.

Table 8. Confusion matrix and prediction performance for two models.

Confusion matrix		Model 1		Model 2	
		Predicted		Predicted	
		Group 1	Group 2	Group 1	Group 2
Actual	Group 1	$TP = 1893$	$FN = 719$	$TP = 2484$	$FN = 128$
	Group 2	$FP = 381$	$TN = 847$	$FP = 98$	$TN = 1130$
Performance indicators					
Recall		83.25%		96.20%	
False alarm rate (FAR)		31.03%		7.98%	
AUC		78.42%		94.17%	

Table 9. Confusion matrix and prediction performance for model 3.

Confusion matrix		Model 3	
		Predicted	
		Group 1	Group 2
Actual	Group 1	$TP = 2193$	$FN = 419$
	Group 2	$FP = 757$	$TN = 471$
Performance indicators			
Recall		74.33%	
False alarm rate (FAR)		61.64%	
AUC		54.27%	

5.3. Comparison results

In the work of Laval and Leclercq (2008), the relaxation process has been successfully modelled. It has been further reformulated by Duret, Ahn, and Buisson (2011) and adopted by Zheng (2014) to analyse the NF's driving behaviour. As Zheng et al. (2013) observed, the NF will generally deviate from the equilibrium state during the anticipation process. They modelled this impact of the anticipation process on the NF by the maximum passing rate with the logic under 70 samples and achieved satisfactory accuracy. Thus, we apply this model to our dataset for comparison purpose. We present the details of this model and its calibration process in the Appendix. For simplification, we name this compared model as model 3 thereafter.

Table 9 presents the confusion matrix and the performance of model 3. This table shows that the prediction accuracy of model 3 is worsened than model 1 and model 2. This result is not surprising because model 3 added a fixed parameter ϵ to reproduce the deviation behaviour of the NF. Consequently, it works well when the NF changes its behaviour. However, as we reported in Table 2, around 30% of the NFs will not change their behaviour (Group 2). Thus, model 3 has an unsatisfactory accuracy for predicting the NF who belongs to group 2, which can be inferred by the large value of FAR in Table 9. This comparison results again highlight that the prediction accuracy can be highly improved by considering the current traffic environment, especially the anticipation-related variables.

5.4. Transferability of the model

To examine the spatial and temporal transferability of our model 2, we additionally select three new sites in Nanjing, as shown in Figure 15. Four trajectory datasets are obtained based on the trajectory extraction method introduced in Section 3. The detailed information of these datasets is presented in Table 10. Specifically, dataset 8 is collected at site 1 to test the performance of our model on the same site but on a different day. A new merging section (site 4) is chosen to evaluate the transferability of our model at different merging locations and times. The other two datasets, one collected at a weaving

Figure 15. Structure of three transferability testing sites.

Table 10. Basic information of transferability testing datasets.

Trajectory datasets	Study site	Date	Time	Type	Weather	Study samples	Group 1 samples	Group 2 samples
Dataset 8	Site 1	23 July 2021	7:45 am-8:45 am	Merging	Sunny	1038	642	441
Dataset 9	Site 4	31 August 2021	8:10 am-9:10 am	Merging	Sunny	945	593	352
Dataset 10	Site 5	6 May 2021	7:30 am-8:30 am	Weaving	Sunny	1370	855	515
Dataset 11	Site 6	13 December 2021	6:30 pm-7:30 pm	Basic road	Night	745	481	273

Table 11. Transferability results of model 2 on different datasets.

Datasets	Recall	False alarm rate (FAR)	AUC
Dataset 8	97.67%	5.59%	96.23%
Dataset 9	94.51%	7.31%	93.91%
Dataset 10	92.27%	9.22%	90.38%
Dataset 11	93.50%	8.73%	91.75%

section, and another collected at a basic road section during the evening peak hour, are used to test whether our model performs well on the different bottlenecks and lighting conditions.

Table 11 gives the prediction results of model 2 on these four trajectory datasets. From Table 11, it can be seen that model 2 achieves even better results on dataset 8 than that on the original dataset. The recall outcome with dataset 9 is marginally lower than that value produced by the original dataset. Fortunately, the FAR value of model 2 using dataset 9 decreases slightly. As a result, the AUC value of model 2 obtained with dataset 9 is 93.91%, which is almost the same as the one obtained with the original dataset (94.17%). The comparison results of dataset 8 and dataset 9 indicate that our model has the potential to predict the NF's behaviour under different merging sites with satisfactory accuracy.

Next, we compare the performance of model 2 with the weaving dataset and the nighttime dataset. Comparing the results in Tables 8 and 11, it can be seen that the prediction accuracy decreases to a reasonable extent when we apply model 2 to dataset 10 and dataset 11. The possible explanation is that the driving behaviours in the weaving section and at nighttime are different from that in the merging section during the daytime. In addition, the original model 2 did not use those data to calibrate. Under such a situation, the small decrease in prediction accuracy is reasonable and acceptable.

6. Conclusion

In this paper, we investigate the response behaviour of the new follower in the target lane (NF) when the lane changer in the adjacent lane (LC) is conducting the anticipation process. Drone videos at three merging sites in Nanjing, China, were recorded. An automatic trajectory extraction method is used to get the vehicle-level trajectory from these drone videos. After that, 3840 available study samples are selected from the whole trajectory datasets. To quantify the NF's behaviour, the ratio between the real wave travel time and the equilibrium time is applied. Consequently, two kinds of NF's response behaviours can be classified: (1) Group 1, the changing of reaction pattern larger than 0.1, indicating that the NF deviates from its initial state; and (2) Group 2, the changing of reaction pattern less than 0.1, indicating that the NF reduces its initial state.

Based on this classification criterion, comprehensive empirical analyses for the NF's response and its relationship with anticipation are conducted. We observe that about 68% of NF samples belong to group 1. The initial reaction values are examined at the two groups. The results show that the NF in group 1 tends to change its behaviour to a more 'timid' pattern even the initial reaction pattern is larger than the equilibrium state. This finding suggests that the NF's behaviour is somehow affected. Next, we detailly describe the impact of these two groups in terms of the gap increasing size and the fluctuation of NF's speed during the anticipation process. We find that the NF exhibits two distinctly different behaviours in group 1 and group 2. Specifically, the NF in group 1 is more likely to produce an extra gap (average 5.36 m), while in group 2 it is more likely to reduce the gap (average 4.65 m). It is interesting to point out that the NL tends to accelerate in group 1 while the NF tends to decelerate during the anticipation process. For group 2, both the NL and the NF tend to decelerate, while the deceleration of the NL is larger than that of the NF.

Furthermore, we analyse some critical factors to see their relationships with the NF's behaviour. Statistical results confirm that the headway (in s) between the NL and NF does not significantly affect the NF's behaviour. However, both the headway between the LC and NF, and the anticipation speed highly correlate with the NF's behaviour. These findings reveal that the deviation behaviour of the NF (group 1) is ascribed to the LC's anticipation behaviour. Therefore, we proposed two binary logistic regression models: (1) the basic model only considers the relation between NL and NF (model 1); and (2) model 1 + anticipation-related variables (model 2). These anticipation-related variables we considered in this study are the anticipation speed, the related speed between NL and LC, the related speed between LC and NF, and the headway between the LC and NF. Several models fit statistics, such as Likelihood ratio, McFadden's R-squared, and BIC all demonstrate that model 2 fits the data more effectively than model 1. Additionally, to further evaluate the prediction capability of these models, the confusion matrix, recall, false alarm rate, and AUC are computed. The results of this comparison conclude that the regression model can predict whether the NF changes its behaviour during the anticipation process with high accuracy. Remarkably, the prediction accuracy can also be significantly increased if we consider the anticipation-related variables. Finally, four additional trajectory datasets are used to test the transferability of the regression model. The results show that the prediction accuracy is still very high when we directly apply the developed model to other trajectory datasets under different bottlenecks and times. It demonstrates that our model has good transferability.

This study provides a comprehensive empirical analysis to understand how the NF's behaviour changes during the anticipation process. More importantly, the binary logistic regression models suggest that the NF's behaviour is highly related to the anticipation behaviour. The results suggest that

when we model the car-following behaviour under the scenario of lane-changing, the impact of the anticipation stage of the lane-changing manoeuvre should be considered. This would provide a better understanding of combing the car-following and lane-changing models into one model. This is ongoing research in our further work. However, this study only focuses on the successful lane-changing sample, and its follower and leader are unchanged during the whole anticipation process. There exist several other lane-changing scenarios in reality, such as the NF may speed up the LC, the NF may also change lane, and the LC even speed up NF in the target lane, in which the relation between the LC and its NFs are expected different. This will be a subject for future research. Finally, the vehicle type has not been considered in this study due to the limited availability of the heavy-vehicle trajectory dataset.

Acknowledgements

We thank Editor, Associate Editor, and the anonymous reviewers for their constructive comments.

Disclosure statement

No potential conflict of interest was reported by the author(s).

Funding

This research was sponsored by the National Natural Science Foundation of China (52272331, 52232021, 71871057).

ORCID

Kequan Chen http://orcid.org/0000-0003-3994-8416
Victor L. Knoop http://orcid.org/0000-0001-7423-3841
Yuxuan Wang http://orcid.org/0000-0001-9153-3512

References

Ahn, S., and M. J. Cassidy. 2007. "Freeway Traffic Oscillations and Vehicle Lane-Changing Maneuvers." The 17th International Symposium on Transportation and Traffic flow Theory, 691–710.

Ali, Y., Z. Zheng, and Md.M Haque. 2018. "Connectivity's Impact on Mandatory Lane-Changing Behaviour: Evidences from a Driving Simulator Study." *Transportation Research Part C: Emerging Technologies* 93: 292–309. doi:10.1016/j.trc.2018.06.008.

Carey, M., C. Balijepalli, and D. Watling. 2015. "Extending the Cell Transmission Model to Multiple Lanes and Lane-Changing." *Networks and Spatial Economics* 15: 507–535. doi:10.1007/s11067-013-9193-7.

Cassidy, M. J., and J. Rudjanakanoknad. 2005. "Increasing the Capacity of an Isolated Merge by Metering its on-Ramp." *Transportation Research Part B: Methodological* 39: 896–913. doi:10.1016/j.trb.2004.12.001.

Chen, D., and S. Ahn. 2018. "Capacity-drop at Extended Bottlenecks: Merge, Diverge, and Weave." *Transportation Research Part B: Methodological* 108: 1–20. doi:10.1016/j.trb.2017.12.006.

Chen, D., J. A. Laval, S. Ahn, and Z. Zheng. 2012b. "Microscopic Traffic Hysteresis in Traffic Oscillations: A Behavioral Perspective." *Transportation Research Part B: Methodological* 46: 1440–1453. doi:10.1016/j.trb.2012.07.002.

Chen, D., J. Laval, Z. Zheng, and S. Ahn. 2012a. "A Behavioral car-Following Model That Captures Traffic Oscillations." *Transportation Research Part B: Methodological* 46: 744–761. doi:10.1016/j.trb.2012.01.009.

Chen, K., P. Liu, Z. Li, Y. Wang, and Y. Lu. 2021. "Modeling Anticipation and Relaxation of Lane Changing Behavior Using Deep Learning." *Transportation Research Record: Journal of the Transportation Research Board* 2675: 186–200. doi:10.1177/03611981211028624.

Duret, A., S. Ahn, and C. Buisson. 2011. "Passing Rates to Measure Relaxation and Impact of Lane-Changing in Congestion." *Computer-Aided Civil and Infrastructure Engineering* 26: 285–297. doi:10.1111/j.1467-8667.2010.00675.x.

Elefteriadou, A. 1996. "A Probabilistic Model of Breakdown at Freeway-Merge Junctions." *Transportation Research Part A: Policy and Practice* 30: 73. doi:10.1016/0965-8564(96)81150-5.

Gao, Jun, Yi Lu Murphey, Jiangang Yi, and Honghui Zhu. 2022. "A Data-Driven Lane-Changing Behavior Detection System Based on Sequence Learning." *Transportmetrica B: Transport Dynamics* 10 (1): 831–848. doi:10.1080/21680566.2020.1782786.

Ghaffari, A., A. Khodayari, N. Hosseinkhani, and S. Salehinia. 2015. "The Effect of a Lane Change on a car-Following Manoeuvre: Anticipation and Relaxation Behaviour." *Proceedings of the Institution of Mechanical Engineers, Part D: Journal of Automobile Engineering* 229: 809–818. doi:10.1177/0954407014547930.

Gipps, P. G. 1986. "A Model for the Structure of Lane-Changing Decisions." *Transportation Research Part B: Methodological* 20: 403–414. doi:10.1016/0191-2615(86)90012-3.

Hou, Y., P. Edara, and C. Sun. 2015. "Situation Assessment and Decision Making for Lane Change Assistance Using Ensemble Learning Methods." *Expert Systems with Applications* 42: 3875–3882. doi:10.1016/j.eswa.2015.01.029.

Jin, W.-L. 2017. "A First-Order Behavioral Model of Capacity Drop." *Transportation Research Part B: Methodological* 105: 438–457. doi:10.1016/j.trb.2017.09.021.

Keane, R., and H. O. Gao. 2021. "A Formulation of the Relaxation Phenomenon for Lane Changing Dynamics in an Arbitrary Car Following Model." *Transportation Research Part C: Emerging Technologies* 125: 103081. doi:10.1016/j.trc.2021.103081.

Kesting, A., M. Treiber, and D. Helbing. 2007. "General Lane-Changing Model MOBIL for Car-Following Models." *Transportation Research Record: Journal of the Transportation Research Board* 1999: 86–94. doi:10.3141/1999-10.

Laval, J. A., and C. F. Daganzo. 2006. "Lane-changing in Traffic Streams." *Transportation Research Part B: Methodological* 40: 251–264. doi:10.1016/j.trb.2005.04.003.

Laval, J. A., and L. Leclercq. 2008. "Microscopic Modeling of the Relaxation Phenomenon Using a Macroscopic Lane-Changing Model." *Transportation Research Part B: Methodological* 42: 511–522. doi:10.1016/j.trb.2007.10.004.

Laval, J. A., and L. Leclercq. 2010. "A Mechanism to Describe the Formation and Propagation of Stop-and-go Waves in Congested Freeway Traffic." *Philosophical Transactions of the Royal Society A: Mathematical, Physical and Engineering Sciences* 368: 4519–4541. doi:10.1098/rsta.2010.0138.

Leclercq, L., V. L. Knoop, F. Marczak, and S. P. Hoogendoorn. 2016. "Capacity Drops at Merges: New Analytical Investigations." *Transportation Research Part C: Emerging Technologies* 62: 171–181. doi:10.1016/j.trc.2015.06.025.

Leclercq, L., N. Chiabaut, J. Laval, and C. Buisson. 2007. "Relaxation Phenomenon after Lane Changing: Experimental Validation with NGSIM Data Set." *Transportation Research Record* 1999: 79–85. doi:10.3141/1999-09.

Li, M., Z. Li, C. Xu, and T. Liu. 2020. "Short-term Prediction of Safety and Operation Impacts of Lane Changes in Oscillations with Empirical Vehicle Trajectories." *Accident Analysis & Prevention* 135: 105345. doi:10.1016/j.aap.2019.105345.

Li, Gen, Zhen Yang, Yiyong Pan, and Jianxiao Ma. 2022. "Analysing and Modelling of Discretionary Lane Change Duration Considering Driver Heterogeneity." *Transportmetrica B: Transport Dynamics*, 1–18. doi:10.1080/21680566.2022.2067599.

Liu, Han, Ye Tian, Jian Sun, and Di Wang. 2022. "An Exploration of Data-Driven Microscopic Simulation for Traffic System and Case Study of Freeway." *Transportmetrica B: Transport Dynamics*, 1–20. doi:10.1080/21680566.2022.2146776.

Ma, L., and S. Qu. 2020. "A Sequence to Sequence Learning Based car-Following Model for Multi-Step Predictions Considering Reaction Delay." *Transportation Research Part C: Emerging Technologies* 120: 102785. doi:10.1016/j.trc.2020.102785.

Marczak, F., W. Daamen, and C. Buisson. 2013. "Merging Behaviour: Empirical Comparison Between two Sites and new Theory Development." *Transportation Research Part C: Emerging Technologies* 36: 530–546. doi:10.1016/j.trc.2013.07.007.

Newell, G. F. 2002. "A Simplified Car-Following Theory: A Lower Order Model." *Transportation Research Part B: Methodological* 36: 195–205. doi:10.1016/S0191-2615(00)00044-8.

Ng, Christina, Susilawati Susilawati, Md Abdus Samad Kamal, and Irene Mei Leng Chew. 2020. "Development of a Binary Logistic Lane Change Model and Its Validation Using Empirical Freeway Data." *Transportmetrica B: Transport Dynamics* 8 (1): 49–71. doi:10.1080/21680566.2020.1715309.

Oh, S., and H. Yeo. 2015. "Impact of Stop-and-go Waves and Lane Changes on Discharge Rate in Recovery Flow." *Transportation Research Part B: Methodological* 77: 8–102. doi:10.1016/j.trb.2015.03.017.

Pan, T., W. H. Lam, A. Sumalee, and R. Zhong. 2016. "Modeling the Impacts of Mandatory and Discretionary Lane-Changing Maneuvers." *Transportation Research Part C: Emerging Technologies* 68: 403–424. doi:10.1016/j.trc.2016.05.002.

Patire, A. D., and M. J. Cassidy. 2011. "Lane Changing Patterns of Bane and Benefit: Observations of an Uphill Expressway." *Transportation Research Part B: Methodological* 45: 656–666. doi:10.1016/j.trb.2011.01.003.

Roque, C., F. Moura, and J. Lourenço Cardoso. 2015. "Detecting Unforgiving Roadside Contributors Through the Severity Analysis of ran-off-Road Crashes." *Accident Analysis & Prevention* 80: 262–273. doi:10.1016/j.aap.2015.02.012.

Schwarz, G. 1978. "Estimating the Dimension of a Model." *The Annals of Statistics* 6 (2): 461–464. doi:10.1214/aos/1176344136.

Smith, S. A. 1985. "Freeway Data Collection for Studying Vehicle Interactions." Federal Highway Administration. Available through the National Technical Information Service.

Nagalur Subraveti, H. H. S., V. L. Knoop, and B. van Arem. 2019. "First Order Multi-Lane Traffic Flow Model – An Incentive Based Macroscopic Model to Represent Lane Change Dynamics." *Transportmetrica B: Transport Dynamics* 7: 1758–1779. doi:10.1080/21680566.2019.1700846.

Wan, Q., G. Peng, Z. Li, and F. H. T. Inomata. 2020. "Spatiotemporal Trajectory Characteristic Analysis for Traffic State Transition Prediction Near Expressway Merge Bottleneck." *Transportation Research Part C: Emerging Technologies* 117: 102682. doi:10.1016/j.trc.2020.102682.

Wang, Y., P. Liu, C. Xu, C. Peng, and J. Wu. 2020. "A Deep Learning Approach to Real-Time CO Concentration Prediction at Signalized Intersection." *Atmospheric Pollution Research* 11: 1370–1378. doi:10.1016/j.apr.2020.05.007.

Yang, M., X. Wang, and M. Quddus. 2019. "Examining Lane Change gap Acceptance, Duration and Impact Using Naturalistic Driving Data." *Transportation Research Part C: Emerging Technologies* 104: 317–331. doi:10.1016/j.trc.2019.05.024.

Yang, D., S. Zheng, C. Wen, P. J. Jin, and B. Ran. 2018. "A Dynamic Lane-Changing Trajectory Planning Model for Automated Vehicles." *Transportation Research Part C: Emerging Technologies* 95: 228–247. doi:10.1016/j.trc.2018.06.007.

Yang, Z., L. Zhibin, L. Pan, and Z. Liteng. 2011. "Exploring Contributing Factors to Crash Injury Severity at Freeway Diverge Areas Using Ordered Probit Model." *Procedia Engineering* 21: 178–185. doi:10.1016/j.proeng.2011.11.2002.

Yuan, J., M. Abdel-Aty, Q. Cai, and J. Lee. 2019. "Investigating Drivers' Mandatory Lane Change Behavior on the Weaving Section of Freeway with Managed Lanes: A Driving Simulator Study." *Transportation Research Part F: Traffic Psychology and Behaviour* 62: 11–32. doi:10.1016/j.trf.2018.12.007.

Zheng, Z. 2014. "Recent Developments and Research Needs in Modeling Lane Changing." *Transportation Research Part B: Methodological* 60: 16–32. doi:10.1016/j.trb.2013.11.009.

Zheng, Z., S. Ahn, D. Chen, and J. Laval. 2011a. "Applications of Wavelet Transform for Analysis of Freeway Traffic: Bottlenecks, Transient Traffic, and Traffic Oscillations." *Transportation Research Part B: Methodological* 45: 372–384. doi:10.1016/j.trb.2010.08.002.

Zheng, Z., S. Ahn, D. Chen, and J. Laval. 2011b. "Freeway Traffic Oscillations: Microscopic Analysis of Formations and Propagations Using Wavelet Transform." *Procedia - Social and Behavioral Sciences* 17: 702–716. doi:10.1016/j.sbspro.2011.04.540.

Zheng, Z., S. Ahn, D. Chen, and J. Laval. 2013. "The Effects of Lane-Changing on the Immediate Follower: Anticipation, Relaxation, and Change in Driver Characteristics." *Transportation Research Part C: Emerging Technologies* 26: 367–379. doi:10.1016/j.trc.2012.10.007.

Zhang, Yue, Yajie Zou, Jinjun Tang, and Jian Liang. 2022. "Long-Term Prediction for High-Resolution Lane-Changing Data Using Temporal Convolution Network." *Transportmetrica B: Transport Dynamics* 10 (1): 849–863. doi:10.1080/21680566.2021.1950072.

Appendix

Here, we present and calibrate the compared model proposed by Zheng et al. (2013). In this model, the formulation for the predicted wave travel time from LC to NF is:

$$\tau_i^{pre}(t) = \tau_i(T_s) + \frac{\varepsilon}{\beta} \ln\left(1 + \frac{\beta t}{w + v_j(T_s)}\right) \tag{A1}$$

where $\tau_i(T_s)$ is the actual wave travel time from the LC to the NF at the start moment of anticipation; ϵ is the speed difference the NF is willing to accept; the β is the NL's acceleration value; $v^j(T_s)$ is the initial speed of the LC.

We use the extracted 3840 anticipation samples, as shown in Section 3, to calibrate Equation (A1). For the parameters $v^j(T_s)$, we adopt the average value; $v^j(T_s) = 7.62$ m/s. Then, we use the same calibration method suggested by Duret, Ahn, and Buisson (2011) to calibrate $\tau^i(T_s)$, ε, and β. The calibration process aims to minimize the Root Mean Squared Error (RMSE) between the real and estimated values. After that, we have the calibrated values; $\tau^i(T_s) = 0.51$s, $\varepsilon = 0.94$ m/s, and $\beta = 1.82$ m/s^2. The RMSE value for calibration is 0.21. The calibrated Equation (A1) provides us with the predicted wave travel time between the LC and the NF at the end moment of anticipation. To identify whether this predicted value belongs to group 1 or group 2, we add the actual wave travel time from the NL to LC (τ^j(t)) on the predicted value of τ *pre i*(*t*). Note that if the wave arrives at the leader at time t^{i-1} and the follower at time t^j, then the wave travel time can be computed as ($t^{i-1} - t^j$). By combining Equations (2), (3), and (A1), we have the identification indicator for this comparison method.

$$\Delta\eta_i = \frac{\tau_i^{pre}(T_e) + \tau_j(T_e)}{\tau} - \eta_i(T_s) \tag{A2}$$